The influence of the norbornene anchor group in Rumediated ring-opening metathesis polymerization:

# Synthesis of linear polymers

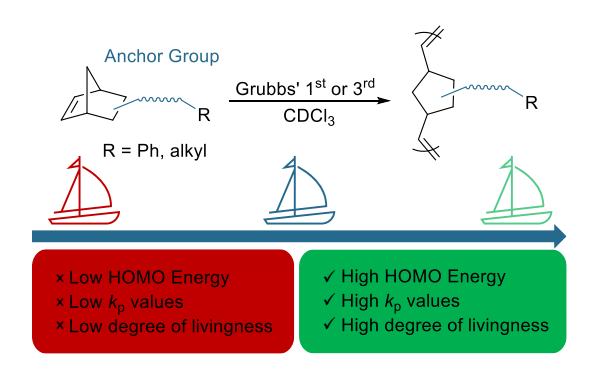
Samantha J. Scannelli, Anshul Paripati, Jeffrey R. Weaver, Clark Vu, Mohammed Alaboalirat, Diego Troya, and John B. Matson\*

Department of Chemistry, Virginia Tech, Blacksburg, VA 24061, United States

Macromolecules Innovation Institute, Virginia Tech, Blacksburg, VA 24061, United States

\*Correspondence: jbmatson@vt.edu

KEYWORDS: Ruthenium catalysts, Propagation, Termination, <sup>1</sup>H NMR spectroscopy, Structure coordinates



For Table of Contents use only

## **ABSTRACT**

Ring-opening metathesis polymerization (ROMP) mediated by Grubbs' first-generation catalyst [G1, (PCy<sub>3</sub>)<sub>2</sub>(Cl)<sub>2</sub>RuCHPh] and Grubbs' third-generation catalyst [G3,

(H<sub>2</sub>IMes)(Cl)<sub>2</sub>(pyr)<sub>2</sub>RuCHPh] can exhibit living characteristics for some monomer classes, most commonly substituted norbornenes. Here we studied how various anchor groups, the series of atoms connecting the polymerizable norbornene unit to a functional group, affect livingness in ROMP in a series of small molecule exo-norbornene monomers. We first designed and calculated the HOMO energy of 61 monomers using density functional theory methods, finding that these energies spanned a range of 25 kcal/mol. We then performed kinetics experiments using <sup>1</sup>H NMR spectroscopy to measure the propagation rate constant  $(k_{p,obs})$  under identical conditions for eight selected monomers with different anchor groups across the range of HOMO energies. We observed a positive correlation between the HOMO energy or the HOMO/LUMO energy gap and measured  $k_{p,obs}$  values for both catalysts, revealing a 30-fold and a 10-fold variation in  $k_{p,obs}$  values across the series for G1 and G3, respectively. Interestingly, we observed a plateau for the three monomers with the highest HOMO energies for G3 catalyst, suggesting that above a certain level, HOMO energy no longer influenced the rate-determining step under the conditions studied here. Chelation studies revealed that only one of the eight monomers showed measurable binding of electron-rich groups on the monomer to the catalyst, but with no apparent effect on  $k_p$ . Finally, we utilized <sup>1</sup>H NMR spectroscopy to measure the rate of catalyst decomposition in the presence of each monomer, a key termination pathway in ROMP. Ultimately, we determined that the anchor group did not substantially affect catalyst decomposition, a proxy for the termination rate constant  $(k_t)$ . In sum, these combined computational and experimental studies collectively demonstrate that livingness in ROMP of exo-norbornene monomers using G1 and G3 catalysts, as measured by relative  $k_p/k_t$ ratios, is primarily controlled by the  $k_p$  of the anchor group, which is correlated with HOMO energy.

#### INTRODUCTION

Polymerizations exhibiting living characteristics, including controllable molecular weights, narrow molecular weight distributions, and retention of chain end functionalities, have been a focus in polymer science for several decades.<sup>1-2</sup> High "livingness" enables the synthesis of welldefined linear polymers including ultrahigh molecular weight polymers<sup>3-4</sup> and (multi)block copolymers.<sup>5-6</sup> Living characteristics also facilitate the construction of precise polymer structures with complex architectures, including cyclic polymers, 7-8 star polymers, 9 and both cylindrical 10-11 and noncylindrical 12-14 bottlebrush polymers, among others. As a result, enhancing livingness across a variety of polymerization methods remains a large focus in the polymer synthesis community. Living polymerizations are defined as chain polymerizations from which chain termination and irreversible chain transfer are absent; additionally, although not required, the rate of initiation is typically higher than that of propagation, creating a constant number of kineticchain carriers throughout the polymerization.<sup>15</sup> While living anionic polymerization in the absence of air, water, or other impurities may represent the only system that fully qualifies as living, 16 several other polymerization methods suppress rates of chain termination and irreversible chain transfer compared with propagation to exhibit living characteristics. <sup>17-18</sup> Chief among them are the reversible-deactivation radical polymerization (RDRP) methods, including atom-transfer radical polymerization (ATRP) and reversible addition-fragmentation chain transfer (RAFT) polymerization.<sup>19-20</sup> Another widely used and versatile polymerization method with living characteristics is ring-opening metathesis polymerization (ROMP).<sup>21</sup> Despite extensive efforts to characterize and enhance livingness in RDRP methods, quantitative studies on the kinetic factors affecting living characteristics in ROMP are lacking.

ROMP is typically initiated and/or mediated by a transition metal catalyst and continues to increase in popularity due to its fast polymerization rates, high functional group tolerance, relative insensitivity to air and water in many cases, and ability to reach full monomer conversion without deleterious side reactions.<sup>21</sup> Most ROMP syntheses with living character utilize Grubbs' 1st generation catalyst [G1, (PCv<sub>3</sub>)<sub>2</sub>(Cl)<sub>2</sub>RuCHPh] or Grubbs' 3<sup>rd</sup> generation catalyst [G3, (H<sub>2</sub>IMes)(Cl)<sub>2</sub>(pyr)<sub>2</sub>RuCHPh], enabling synthesis of multiblock polymers and polymers with complex topologies.<sup>22</sup> For example, Kilbinger employed ROMP using G3 catalyst to synthesize heptablock copolymers with degradable linkages in alternating blocks, 23 and we recently synthesized decablock bottlebrush polymers to demonstrate the efficiency of a sequential addition of macromonomers (SAM) approach to ROMP.<sup>12</sup> Xie and coworkers synthesized AB<sub>2</sub> star polymers with G1 catalyst, <sup>24</sup> which has lower initiation and propagation kinetics than G3 catalyst but is simpler, cheaper, and more bench stable.<sup>25</sup> Despite these successes, close examination of the data in these and other papers reveals limits to the living character in ROMP, as evidenced by increasing dispersity values with each additional block and low molecular weight tails in the size exclusion chromatography (SEC) traces due to prematurely terminated chains. Thus, a comprehensive picture of the factors that influence living character in ROMP is critical to address these limitations, enabling synthesis of precise polymer structures to derive structure-property relationships in linear (multi)block copolymers and complex polymer topologies.

In any polymerization with living characteristics, the propagation rate, which is largely determined by the propagation rate constant  $(k_p)$ , must be much higher than that of any chain-breaking reaction, i.e., chain transfer or termination (we focus here on termination,  $k_t$ ). Matyjaszewski ranked the livingness of various polymerization systems by comparing  $k_p/k_t$  ratios among different polymerization systems, where higher  $k_p/k_t$  ratios indicate greater livingness. <sup>17</sup> In

the case of ROMP of substituted norbornenes initiated by G1 or G3 catalyst to make linear polymers, there is high living character due to three factors: 1)  $k_p$  is high—polymerizations are typically complete within a few minutes for G3 and several minutes to a few hours for G1; 2) chain transfer is absent; and 3) catalyst decomposition pathways, which collectively determine  $k_t$ , are relatively low.

In 2016 we hypothesized that  $k_p$ , and thus the  $k_p/k_t$  ratio, could be enhanced in ROMP by tuning monomer reactivity. We discovered that the anchor group, the series of atoms connecting the polymerizable unit to the side chain, had an unexpectedly large effect on  $k_p$ . While it was already well known that *exo*-norbornene monomers underwent ROMP 10–100-fold faster than *endo*-norbornene monomers, his work revealed a 5–10-fold increase in  $k_p$  among a set of three *exo*-norbornene monomers with polymerization initiated by G3 catalyst. This increase in  $k_p$  was achieved by changing the anchor group from an imide to an ester, leading to an increase in the maximum obtainable bottlebrush polymer backbone degree of polymerization from ~100 to ~800 in a pair of identical macromonomers with varying anchor groups. Computational studies in this original work indicated that the rate differences were correlated with differences in electronic structure among the various anchor groups, highlighting how rational selection of the anchor group could enable high macromonomer conversion and improve livingness in ROMP, which is vital for making precise bottlebrush polymers.

In our earlier work on the effects of the anchor group on ROMP, we studied three common anchor groups, and we observed a positive correlation between the energy of the monomer HOMO, localized on the reactive olefin, and  $k_p$ . Here we aimed to apply a combined computational/experimental approach to extensively study the effect of the anchor group in ROMP of small molecule *exo*-norbornene monomers on  $k_p$ , catalyst decomposition (a proxy for  $k_t$ ), and

the resulting living character of this polymerization method (Scheme 1). We hypothesized that computational methods could be applied to a wide range of monomer structures to suggest anchor groups with varying electronic structures, and that experimental kinetic measurements on a selected group of these monomers using both G1 and G3 catalysts would reveal how HOMO energy relates to living character in ROMP.

**Scheme 1.** Representative scheme of ROMP of monomers with various anchor groups.

$$\begin{array}{c|c} & \text{anchor} \\ & \text{group} \\ & \text{energy} \\ & \text{affects } k_p \\ & \text{R} = \text{Ph, alkyl} \end{array} \\ \begin{array}{c} & \text{G1 or G3 catalyst} \\ & \text{ROMP} \\ & & \text{R} \end{array}$$

#### RESULTS AND DISCUSSION

To investigate the relationship between HOMO energy and  $k_p$ , we designed 61 different norbornene-based monomers with varying anchor groups (Figure S1). We then set out to 1) calculate the HOMO energy for each of them, 2) select several to synthesize across a range of HOMO energies, and 3) measure their  $k_p$  values and effects on catalyst decomposition ( $k_t$ ) in ROMP using both G1 and G3 catalysts under standardized conditions. We previously showed, out of three macromonomers, that higher HOMO energies led to higher polymerization rates.<sup>26</sup> Therefore, we hypothesized that the  $k_p$  in polymerizations mediated by G1 and G3 catalysts would be commensurate with HOMO energy.

# HOMO Energy Calculations

To obtain HOMO energies for a large number of monomers, we restricted our calculations to relatively small structures. All monomers were designed with a norbornene on one end as the

polymerizable unit and a phenyl or alkyl group on the other, ensuring the differences in the HOMO energies were due to the anchor group (Figure S1). The HOMO energies were then calculated from optimized geometries of all 61 monomers using density functional theory (B3LYP method and 6-31G(d) basis set). 30-31 Coordinates of all monomer structures and all HOMO energies are shown in the Supporting Information. The HOMO energies ranged from -161 to -136 kcal/mol. We synthesized several of these monomers, but many precipitated out during ROMP, especially those with NH bonds. Ultimately, we selected a total of eight monomers for further experimental testing (Figure 1), all of which underwent ROMP without precipitation in initial tests. The selected monomers had HOMO energies ranging from -161 to -145 kcal/mol. We note that we did synthesize and ROMP some monomers in the range from -145 to -136 kcal/mol, but all precipitated during polymerization, preventing inclusion in the final study. Optimized geometries and HOMO energies of the eight selected monomers were recalculated using a higher level of theory (M06-2X method and def2-TZVP basis set)<sup>32-33</sup> for a better understanding of their electronic structures. At this higher level of theory, the HOMO energies ranged from -197 to -186 kcal/mol. The ROMP kinetics of these monomers were then extensively studied experimentally.

**Figure 1**. Monomers with various anchor groups (blue) synthesized and polymerized via ROMP. All monomers exhibited exo (x prefix) or exo-exo (xx prefix) stereochemistry. Letters identify structural components of the anchor group from left to right (x = methylene/methyl, x = oxygen, x = phenyl, x = ester with carbonyl on the left, x = ester with carbonyl on the right, x = imide). Subscripts indicate the number of times that component is repeated.

# <sup>1</sup>H NMR Kinetic Analysis

All monomers were polymerized in the presence of G1 and G3 catalysts, separately, under the same conditions to investigate whether the effects of the anchor groups differed depending on the catalyst. To avoid solvent removal before NMR spectroscopic analysis, we used purified CDCl<sub>3</sub> as the solvent, and all polymerizations were carried out under air and at room temperature at a monomer concentration of 20 mM, targeting a degree of polymerization of 100. Aliquots were taken from the reaction mixture at pre-determined time points and injected into vials containing an excess of ethyl vinyl ether in CDCl<sub>3</sub> to terminate the reaction. Conversion of norbornene monomers 1–8 was monitored by <sup>1</sup>H NMR spectroscopy by comparing the integration of the polymer backbone olefin protons to the olefin protons of the monomer.

ROMP can be considered a pseudo-first order reaction;<sup>34</sup> therefore, these data were fit to first-order kinetic plots. Representative  $^{1}$ H NMR spectra and kinetics plots are shown in Figure 2 for an example monomer xx-IM<sub>2</sub>E'P (8) with either G1 (A–B) or G3 (C–D) as the catalyst; plots for all other monomers can be found in the Supporting Information (Figures S20–S51). Averaged  $k_{p,obs}$  and half-life values were determined over at least three kinetics runs for each monomer. After quenching the reaction following removal of the final aliquot, the reaction mixture was concentrated to obtain the final polymer. SEC analysis of the final polymers showed that molecular weights were close to expected values, and all polymers showed monomodal peaks with low dispersities (Figures S52-S67). All rate and SEC data are shown in Table 1.

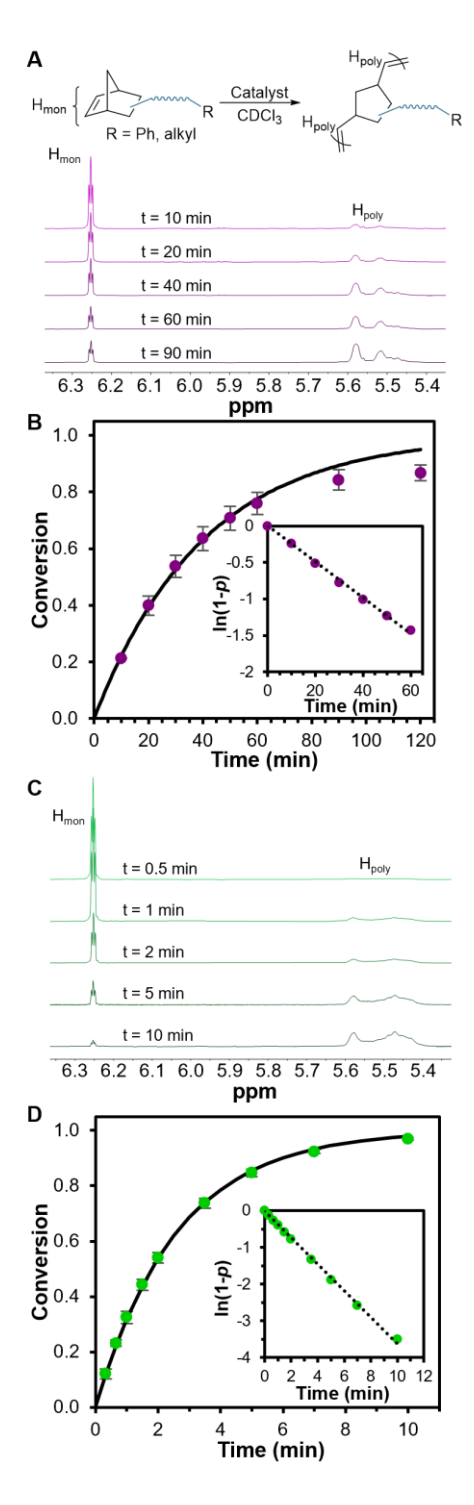


Figure 2. (A) Representative spectra for <sup>1</sup>H NMR kinetics experiment of the ROMP of monomer xx-IM<sub>2</sub>E'P (8) with G1 catalyst. As the polymerization proceeds, the norbornene olefin resonance at ~6.26 ppm decreases in relative area, and the polymer backbone resonance at 5.4–5.6 ppm increases in relative area. (B) Kinetic analysis of monomer xx-IM<sub>2</sub>E'P (8) in CDCl<sub>3</sub> with G1 catalyst at a [monomer]/[G1] ratio of 100:1 and [monomer] = 20 mM. The solid line represents the fit to the averaged conversion data based on the equation  $p = 1 - e^{(-k_p t)}$  where p = fractional

conversion. (C) Representative spectra for <sup>1</sup>H NMR kinetics experiment of the ROMP of monomer xx-IM<sub>2</sub>E'P (8) with G3 catalyst. As the polymerization proceeds, the norbornene olefin resonance at ~6.26 ppm decreases in relative area, and the polymer backbone resonance at 5.4–5.6 ppm increases in relative area. (D) Kinetic analysis of monomer xx-IM<sub>2</sub>E'P (8) in CDCl<sub>3</sub> with G3 catalyst at a [monomer]/[G3] ratio of 100:1 at [monomer] = 20 mM. The solid line represents the fit of each data set generated using experimentally determined  $k_p$  values based on the equation  $p = 1 - e^{(-k_p t)}$ .

**Table 1.** HOMO energies, HOMO/LUMO gap energies, polymerization kinetics, and polymer characterization for ROMP of monomers 1–8

Anchor Group	HOMO Energy <sup>a</sup> (kcal/mol)	HOMO/ LUMO Gap <sup>a</sup> (kcal/mol)	Catalyst	$k_{ m p,obs} ({ m min}^{ ext{-}1})$	t <sub>1/2</sub> (min)	$M_{ m n,SEC}^{b}$ (kDa)	$M_{ m n,expected}^c$ (kDa)	Đ
<i>x</i> -MOMP (1)	-186	213	Gl	$0.271 \pm 0.008$	$2.6 \pm 0.2$	26	21	1.04
<i>x</i> -ME'P ( <b>2</b> )	-188	214		$1.4 \pm 0.1$	$0.51 \pm 0.04$	25	23	1.07
<i>x</i> -EMP ( <b>3</b> )	-190	211		$0.055 \pm 0.006$	$13 \pm 1$	19	23	1.15
<i>xx</i> -IMP ( <b>4</b> )	-193	215		$0.049\pm0.007$	$14\pm1$	22	25	1.05
$xx-IM_6$ (5)	-195	217		$0.030\pm0.007$	$24\pm 6$	31	25	1.06
xx-IMEM <sub>2</sub> E'P (6)	-196	217		$0.020 \pm 0.0008$	$35 \pm 1$	48	37	1.05
xx-IMEMP (7)	-196	218		$0.034\pm0.004$	$20\pm3$	35	31	1.05
xx-IM <sub>2</sub> E'P (8)	-197	218		$0.027 \pm 0.003$	$27\pm4$	32	31	1.04
<i>x</i> -MOMP (1)	-186	213	G3	$3.7 \pm 0.3$	$0.19 \pm 0.02$	23	21	1.04
<i>x</i> -ME'P ( <b>2</b> )	-188	214		$3.3 \pm 0.6$	$0.22 \pm 0.04$	24	23	1.06
<i>x</i> -EMP ( <b>3</b> )	-190	211		$4.8 \pm 0.9$	$0.17 \pm 0.01$	28	23	1.07
<i>xx</i> -IMP ( <b>4</b> )	-193	215		$0.54 \pm 0.03$	$1.31 \pm 0.07$	22	25	1.01
$xx-IM_6$ (5)	-195	217		$0.66 \pm 0.05$	$1.06 \pm 0.07$	30	25	1.01
xx-IMEM <sub>2</sub> E'P (6)	-196	217		$0.40\pm0.04$	$1.66 \pm 0.06$	41	37	1.02
xx-IMEMP (7)	-195	218		$0.60 \pm 0.04$	$1.15\pm0.07$	37	31	1.01
xx-IM <sub>2</sub> E'P (8)	-197	218		$0.38 \pm 0.02$	$1.8 \pm 0.1$	39	31	1.01

<sup>a</sup>Calculated using M06-2X method and def2-TZVP basis set. <sup>32-33</sup> <sup>b</sup>Measured on samples removed after the final aliquot of the kinetics run by SEC in THF at 30 °C with multiangle light scattering and refractive index detectors. <sup>c</sup>Determined using the equation  $M_{n,expected}$  = monomer molar mass \* ([monomer]/[catalyst])<sub>0</sub>.

G1 catalyst mediates ROMP with lower  $k_p$  values than G3 catalyst,<sup>35</sup> so the rate constants observed with G1 catalyst were generally 10–20-fold lower than the rate constants observed with G3 catalyst. We noticed that some monomers, mainly those with low  $k_{p,obs}$  values, did not reach full monomer conversion when polymerized with G1 catalyst. Therefore, we calculated  $k_{p,obs}$  in these cases from conversion data only up to ~80% to ensure good first-order kinetics fits. Most monomers had half-lives greater than 2 min with G1 catalyst, with half-lives for imide-based monomers 4–8 in the range of 14–35 min. In contrast, all monomer half-lives were less than 2 min with G3 catalyst, with the fastest monomers showing half-lives in the range of 10 s. Additionally, the ROMP of these eight monomers with either catalyst showed at least an order of magnitude difference between the monomers with the highest and lowest  $k_{p,obs}$  values; however, the spread within the series was larger for G1 catalyst (70-fold) compared with G3 catalyst (10-fold).

Our group previously found that differences in the rate of ROMP of macromonomers arose primarily from differences in electronic structure among the various anchor groups. <sup>26</sup> Additionally, investigations into the mechanism of ROMP from Guironnet and coworkers showed that the rate-determining step of ROMP with norbornene-based monomers was the formation of the metallacyclobutane (as opposed to the subsequent collapse of the metallacyclobutane to reorganize the double bonds or the coordination/decoordination of pyridine to the catalyst), <sup>36</sup> further suggesting the importance of the energy of the monomer HOMO, centered on the olefin, in determining  $k_p$ . Metallacyclobutane formation is a cycloaddition, which employs the  $\pi$  electrons of the olefin substrate to form a bond with the catalyst. These  $\pi$  electrons of the olefin correspond to the HOMO, however, other orbital interactions are possible in the rate-determining formation of the metallacyclobutane.

A detailed computational study by Suresh and Koha of frontier molecular orbitals in olefin metathesis with G1 revealed that at the transition state leading to metallacyclobutane formation, the  $\pi$  electrons in the olefin HOMO interact with the empty  $\pi^*$  and d orbitals of the Ru=C bond, but there is also a backbonding interaction of the  $\pi$  orbital of the Ru=C bond with the  $\pi^*$  orbital of the olefin (LUMO).<sup>37</sup> (We note that the  $\pi^*$  orbital of the olefin does not always correspond to the absolute lowest-energy unoccupied molecular orbital of the substrate. In this paper, we use LUMO to refer to the  $\pi^*$  orbital of the olefin.) Therefore, we examined the HOMO, LUMO, and HOMO/LUMO energy gap for our eight monomers and compared the  $k_{\rm p,obs}$  values with these calculated energies. Monomers with both high HOMO and low olefin-centered LUMO energies should facilitate the interaction with the metal carbene during the formation of the metallacyclobutane, increasing reactivity and resulting in higher  $k_{\rm p,obs}$  values than monomers with low HOMO and high olefin-centered LUMO energies.

A positive correlation between the HOMO energy and the  $k_{p,obs}$  value of each monomer was found for both catalysts (Figure 3). An inverse correlation was found when comparing the HOMO/LUMO energy gaps and the  $k_{p,obs}$  values for each monomer (Figure S68), suggesting the importance of multiple orbital interactions in the rate-determining step of ROMP. In other words, both HOMO energy and HOMO/LUMO energy gap were reasonable predictors of  $k_p$ , so we focus here on the HOMO energies. However, the trend was not completely linear for either catalyst; in fact, we observed a plateau for monomers with HOMO energies above -190 kcal/mol when G3 catalyst was used. This plateau suggests that the influence of the anchor group on the polymerization rate of monomers is lost at high HOMO energies; in other words, the anchor group may no longer influence the rate-determining step once its HOMO level exceeds this energy. However, it is possible that for ROMP with G3 catalyst under conditions that experience low  $k_p$ 

such as large macromonomers<sup>38</sup> or potentially in non-ideal solvents,<sup>39</sup> a  $k_p$  difference among ester and ether-based anchor groups 1–3 may be observed. We also considered steric differences among the various monomers and their impact on metallacyclobutane formation but no significant changes in metallacyclobutane geometries were observed (Figure S69), suggesting steric constraints in the formation of this intermediate are comparable among monomers.

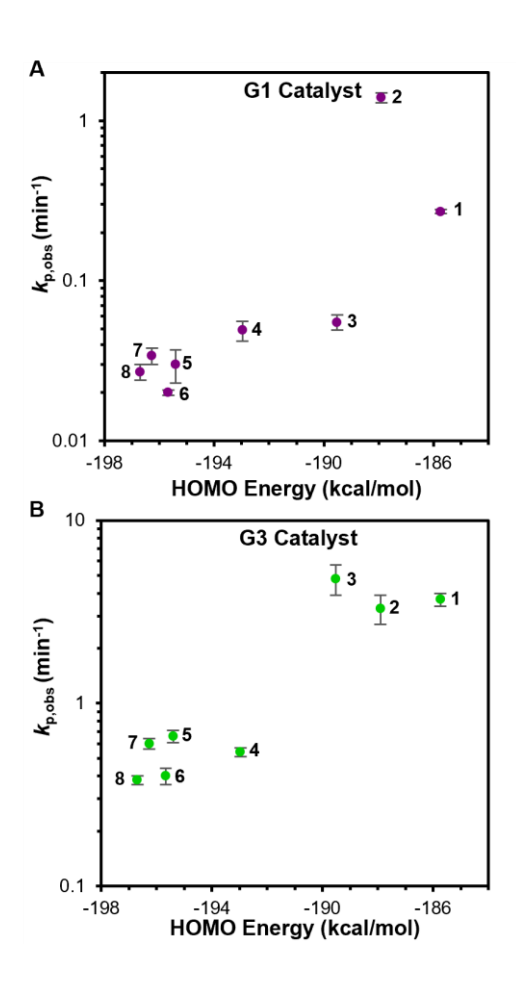


**Figure 3**. Measured  $k_{p,obs}$  versus HOMO energy for monomers **1–8** with G1 catalyst (A) and G3 catalyst (B).

When using G1 catalyst, which exhibited a lower  $k_p$  for all monomers, we observed larger differences between the three monomers with HOMO energies above -190 kcal/mol (1–3), suggesting that the anchor group influences metallacyclobutane formation for these monomers

with G1 catalyst. Although larger rate differences among monomers 1–3 were found with G1 than with G3 catalyst, we observed an unexpectedly higher  $k_{p,obs}$  in monomer x-ME'P (2) compared with monomer x-MOMP (1). The HOMO energies of x-MOMP (1) and x-ME'P (2) are likely within the accuracy of the DFT methods, but these results may also suggest additional factors that influence  $k_p$  beyond the HOMO energy. Overall, for both catalysts  $k_{p,obs}$  generally increased with increasing HOMO energy.

#### Chelation Effect

Certain anchor groups, mostly those containing carbonyls, may be able to chelate to Ru olefin metathesis catalysts, which can impact the polymerization rates of various monomers.<sup>36</sup> We therefore conducted <sup>1</sup>H NMR spectroscopy experiments, based on previously reported procedures by Grubbs and coworkers,<sup>40</sup> to identify the presence of chelation. These experiments rely on measuring the amount of pyridine in solution during the polymerization, a method originally established by Guirronet and coworkers.<sup>34</sup> Chelation studies were only done for G3 catalyst since G1 catalyst does not contain a pyridine ligand. However, we expect that the trends would be similar between the two catalysts due to their similar structures and reactivity profiles.<sup>41</sup>

Samples containing G3 catalyst and 10 equiv of monomers 1–8 were prepared in CDCl<sub>3</sub>. Targeting a small degree of polymerization (10) allowed for polymerizations to reach their final propagating structure (a terminal Ru-alkylidene) prior to <sup>1</sup>H NMR analysis while retaining sufficient signal. All polymerizations were expected to have one pyridine free in solution, as the catalyst loses the first ligand upon dissolution.<sup>34</sup> However, the binding of the second pyridine ligand should depend on anchor group structure, where chelating anchor groups would compete with binding of the second pyridine to the metal center, at least to some measurable degree

(Scheme 2). Free pyridine in solution was measured by comparing the integration of the *ortho* protons of the free pyridine at about 8.7 ppm relative to the alkylidene proton of the propagating catalyst species (Ru=CH-poly) near 18.5–19.0 ppm. Therefore, in this assay, polymers without chelating anchor groups show one pyridine in solution, with an integral value of 2 for the two *ortho* protons (the other pyridine binds to the metal center). Conversely, polymers with chelating anchor groups show more than one pyridine in solution, with an integral value of more than 2 for the *ortho* protons (full chelation would show two free pyridines and therefore an integral value of 4). Monomers 1–3 have two possible regioisomers for the propagating alkylidene structure that can affect chelation; we envisioned that our experiments would reveal a mixture of chelated and nonchelated species with a free pyridine integral value near 3.

**Scheme 2**. Examples of propagating polymer chains with chelating and non-chelating anchor groups and their expected free pyridine integration values.

Chelating

Because monomers x-ME'P (2), xx-IMEM<sub>2</sub>E'P (6), and xx-IM<sub>2</sub>E'P (8) experienced resonance overlap between monomer protons and the *ortho* protons of the bound pyridine, in this study we compared the relative NMR integrations of just the free pyridine to the Ru-alkylidene

proton. It is worth noting that monomers 1-3 have two possible regionsomers for the propagating alkylidene structure that can affect chelation. Regardless, any form of chelation would still be observed during the experiments to reveal a mixture of chelated and nonchelated species. Out of all eight monomers tested, monomer x-EMP (3) was the only one to show any chelation of the propagating polymer structure, with a free pyridine integration value of 3.0, implying a mixture of chelated and nonchelated species during polymerization. The broad resonance also suggested the rapid and reversible chelation of the polymer chain (Figure S72). ROMP of all other monomers had free pyridine integrations close to 2, so when comparing the integration of the free pyridine to the  $k_{p,obs}$  of each monomer, there was no correlation between the two variables (Figure 4). Although we did not specifically measure chelation for G1 due to a lack of pyridines on this catalyst, the chelation observed in the ROMP of monomer x-EMP (3) may explain the surprisingly low  $k_{p,obs}$  found with G1 catalyst compared to G3 catalyst. The  $k_{p,obs}$  of monomer x-EMP (3) more closely aligns with monomers x-MOMP (1) and x-ME'P (2) with G3 catalyst, but with imide-based monomers 4–8 with G1 catalyst, despite the structural similarities between monomers x-MOMP (1), x-ME'P (2), and x-EMP (3). Therefore, we speculate based on these results that the chelating anchor group of monomer x-EMP (3) affects  $k_p$  with G1 more than with G3 catalyst, decreasing the rate compared with a hypothetical non-chelating monomer with the same HOMO energy. Regardless, we found no correlation between chelation and  $k_{p,obs}$  across all monomers in this study, which further emphasizes the relationship between HOMO energy and propagation rate.

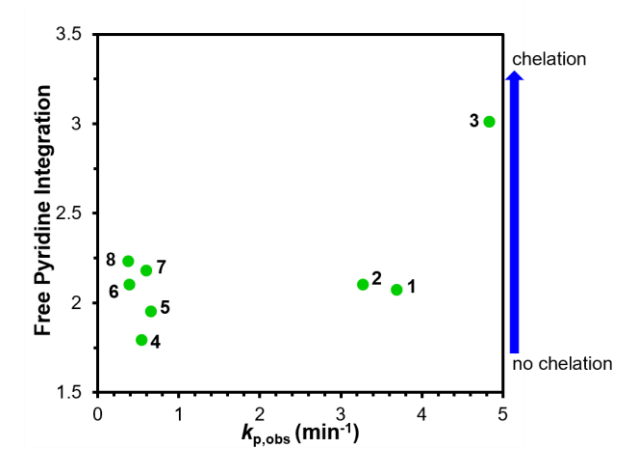


**Figure 4**. Free pyridine <sup>1</sup>H NMR integration values versus  $k_{p,obs}$  of each monomer after polymerization with G3 catalyst. Error bars on integral values are estimated to be  $\pm$  10 % due to errors associated with integrating small peaks. Polymerizations were carried out in CDCl<sub>3</sub> with G3 at a [monomer]/[G3] ratio of 10:1 and [G3] = 40 mM.

Results from our chelation studies were in line with similar monomers reported by Grubbs and Guironnet.  $^{36, 40}$  Both observed no chelation in the ROMP of *exo*-norbornene imide monomers, i.e., those with anchor groups similar to monomers **4–8**. In addition, Grubbs observed no chelation in the ROMP of an ether-containing monomer with an anchor group that resembled monomer x-MOMP (1) here, and both Grubbs and Guironnet found chelation in the ROMP of monomers with ester-based anchor groups similar in structure to monomer x-EMP (3). They also did not notice any effects of chelation on  $k_p$  for *exo*-norbornene monomers. We considered the possibility that initiation rates could influence the observed propagation rate; however, Guironnet recently showed that initiation rates were similar among different *exo*-norbornene monomers.  $^{36}$ 

# Catalyst Decomposition and Livingness in ROMP

To further evaluate how the anchor group influences livingness in ROMP, we set out to estimate relative catalyst decomposition rates as a proxy for  $k_t$  values for G1 and G3 catalysts with the eight different monomers. Direct measurement of  $k_t$  during the polymerization in these samples

was experimentally difficult because  $k_p$  is too fast for data collection during the polymerization by NMR spectroscopy. The earliest NMR spectrum we were able to acquire with sufficient alkylidene signal was about 2 min into the polymerizations, which is enough time for monomer x-ME'P (2) with G1 and monomers 1-3 with G3 catalyst to reach near-complete conversion to polymer. Therefore, we were unable to measure catalyst decomposition during the polymerization for these monomers. Analysis by UV-vis was also unusable because both catalysts have featureless UV-vis spectra after initiation. Instead, we used <sup>1</sup>H NMR spectroscopy to estimate the % catalyst decomposition after near-complete monomer consumption. We speculate that more termination pathways are available when monomer is present because some decomposition pathways may only be accessible when the catalysts are in the metallacyclobutane form and not in the alkylidene form.<sup>42</sup> To ensure that each monomer was tested in an equal fashion, we decided to measure % catalyst decomposition after a consistent number of propagation half-lives for each catalyst: We measured all spectra after 12 propagation half-lives for G3 because it took 2 min to acquire a <sup>1</sup>H NMR spectrum with sufficient resolution for the fastest monomers, equivalent to 12 half-lives. For G1 catalyst, we measured all spectra after 4 half-lives because the fastest monomer with G1 [x-ME'P (2) reaches 4 half-lives in 2 min, and 12 half-lives would have been extremely long for the slowest monomers.

Samples containing catalyst (G1 or G3) and an internal standard (phenanthrene or anthracene, respectively) were prepared in CDCl<sub>3</sub>. We used <sup>1</sup>H NMR spectroscopy to measure the integration of the benzylidene proton on G1 and G3 catalysts relative to an internal standard proton before monomer addition. Next, 100 equiv of monomer was added to the NMR tube, initiating the polymerization. For each monomer, we acquired a <sup>1</sup>H NMR spectrum after 4 propagation half-lives for G1 and 12 propagation half-lives for G3 catalyst, which allowed us to measure the

decrease in the integration of the benzylidene/alkylidene proton and to monitor catalyst decomposition over time, which we report as estimated  $k_{t,obs}$  values.

We observed small differences in  $k_{t,obs}$  values across all monomers with either G1 or G3 as the catalyst (Figure 5). For G1 catalyst,  $k_{t,obs}$  values ranged from about 0.006 to 0.015 min<sup>-1</sup>, while rates ranged from 0.006 to 0.018 min<sup>-1</sup> for G3 catalyst. However, there were no clear trends, and the error in these measurements was fairly large due to the fairly small amounts of catalyst decomposition in these experiments and the error associated with precisely integrating small signals. To further investigate  $k_t$ , we estimated the % dead chains from the SEC traces of the final polymers. The slight variations in D values and low molecular weight tails in the SEC traces suggested different amounts of chain termination for each monomer. Therefore, we deconvoluted the low molecular weight tails of the SEC traces by assuming a Gaussian distribution, <sup>43</sup> and found little variation in the % dead chains for monomers 1–8 with both catalysts (Figures S94–109). From these results, we conclude that the anchor group did not affect  $k_{t,obs}$  to a measurable extent for either catalyst. Thus, while other variables such as solvent influence  $k_t$ , <sup>39, 44-45</sup> the anchor group only significantly affects the  $k_p$  component of the  $k_p/k_t$  ratio, at least under the conditions used here. These results are consistent with HOMO localization on the reactive norbornene olefin, which would impact  $k_p$ , whereas termination events occur in the metallacyclobutane form or alkylidene form of the catalyst once the norbornene olefin has reacted.

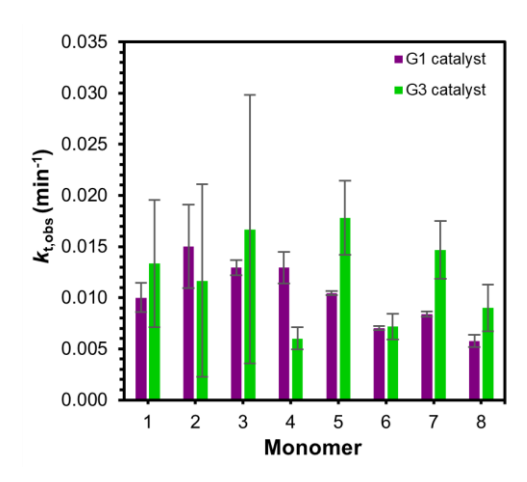


**Figure 5**. Experimentally determined  $k_{t,obs}$  values for G1 (purple) and G3 (green) catalysts with different monomers. All  $k_{t,obs}$  values were estimated using the equation  $k_{t,obs}$  = (fraction catalyst decomposition)(time to x propagation half-lives)<sup>-1</sup> (x = 4 for G1 and 12 for G3) where decomposition was monitored using <sup>1</sup>H NMR spectroscopy. Polymerizations were carried out in CDCl<sub>3</sub> with a [monomer]/[catalyst] ratio of 100:1 and [catalyst] = 0.6 mM.

Using the  $k_{p,obs}$  and  $k_{t,obs}$  results, we were then able to generate relative  $k_p/k_t$  ratios for each monomer with both catalysts, where higher  $k_p/k_t$  ratios indicate greater living character. We used the  $k_{p,obs}$  values measured from our kinetics experiments and the  $k_{t,obs}$  values measured from catalyst decomposition studies to calculate the ratios, and then compared the values for each monomer. While these ratios are not true  $k_p/k_t$  ratios because  $k_{p,obs}$  and  $k_{t,obs}$  were measured under different conditions, they capture the relative differences between the anchor groups (Figure 6).

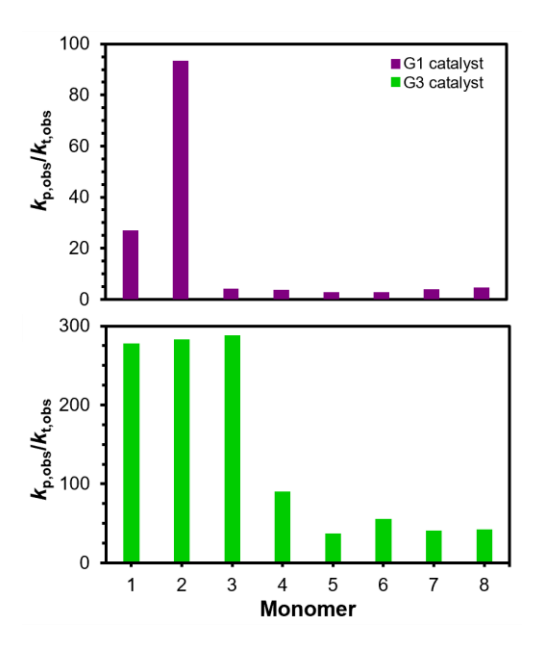


**Figure 6**. Relative  $k_p/k_t$  ratios for each monomer with either G1 (purple) or G3 (green) catalysts determined from the  $k_{p,obs}$  values (measured from the kinetics studies on propagation) and the  $k_{t,obs}$  values (estimated from the catalyst decomposition studies).

For polymerizations mediated by G1 catalyst, we observed at least a 10-fold difference in the  $k_p/k_t$  ratios between two groups: 1) monomers x-MOMP (1) and x-ME'P (2) with high  $k_{p,obs}$  and, 2) monomers 3–8 with low  $k_{p,obs}$  values. This order of magnitude difference in the  $k_p/k_t$  ratios is driven by the higher  $k_{p,obs}$  values for monomers x-MOMP (1) and x-ME'P (2), as the catalyst decomposition rate was similar across all monomers. Anchor group choice is clearly crucial for polymerizations mediated by G1 catalyst, where only monomers x-MOMP (1) and x-ME'P (2) displayed a high enough  $k_p$  to maintain a high degree of livingness during ROMP to DP=100.

Polymerizations mediated by G3 catalyst showed two distinct groups as well. The high  $k_{p,obs}$  monomers (1–3) showed at least a 4-fold higher  $k_p/k_t$  ratio compared to the monomers with lower  $k_{p,obs}$  (4–8). The relative  $k_p/k_t$  values for monomers 1–3 were all quite similar and within the error of the measurements. In contrast, monomer x-ME'P (2) was the most living monomer with G1 by a substantial margin. Therefore, among these anchor groups, we conclude that the ester

anchor group used in monomer x-ME'P (2) is the most living for ROMP under conditions that experience low  $k_p$  (i.e., with G1 catalyst or with sterically demanding monomers). In contrast, monomers 1–3 show similar levels of livingness with G3 catalyst under higher  $k_p$  conditions utilizing small molecule monomers in a good solvent. Finally, the  $k_p/k_t$  ratios for polymerizations with G3 catalyst were 3–20-fold higher than those with G1 catalyst, consistent with the higher activity of G3 catalyst. These results suggest that while many anchor groups demonstrate a reasonably high degree of livingness for G3 catalyst, anchor group choice is more critical when using G1 catalyst, where only monomers x-MOMP (1) and x-ME'P (2) display high livingness.

#### CONCLUSIONS

In summary, we find that the anchor group significantly affects the propagation rate ( $k_p$ ) but not the termination rate ( $k_t$ ) in ROMP of small molecule *exo*-norbornene monomers. The calculated HOMO energies of monomers with various anchor groups were positively correlated with the  $k_{p,obs}$  of the polymerizations initiated by either G1 or G3 catalyst, suggesting that monomers with higher HOMO energies exhibit greater reactivity in ROMP than monomers with lower HOMO energies. However, we observed an upper limit in  $k_{p,obs}$  for polymerizations of this monomer set with G3 catalyst, where a plateau in rate was observed for monomers with HOMO energies above -190 kcal/mol, suggesting that the anchor group no longer affected the rate-determining step once above this limit. Chelation to G3 catalyst was also measured, but it had little impact on  $k_{p,obs}$  in the eight *exo*-norbornene monomers studied here. Therefore, in the synthesis of linear polymers by ROMP using G3 catalyst in a good solvent, anchor group choice affects  $k_p$ , but becomes inconsequential above a certain HOMO energy level.

Additionally, the anchor group had little effect on  $k_t$  for both G1 and G3 catalysts. The estimated  $k_{t,obs}$  values were fairly uniform across all monomers for both catalysts, suggesting that  $k_t$  is not heavily affected by the anchor group. This result is consistent with decomposition during ROMP occurring after the norbornene olefin, where the HOMO is localized, has reacted to form a metallacyclobutane and then a propagating alkylidene. Combining  $k_{t,obs}$  and  $k_{p,obs}$  results, we determined that the anchor group significantly affected the  $k_p/k_t$  ratios, where higher  $k_p/k_t$  ratios indicate greater livingness. Large differences in the  $k_p/k_t$  ratios were driven by the differences in  $k_p$  because little variation was found for  $k_t$  with the different monomers. Monomers with the highest  $k_{p,obs}$  values [monomer x-ME'P (2) with G1 and monomers x-MOMP (1), x-ME'P (2), and x-EMP (3) with G3] had the highest  $k_p/k_t$  ratios and therefore the highest degree of livingness. Ultimately, anchor group choice greatly influences the rate and livingness of ROMP with G1 and G3 catalysts. When synthesizing more complex topologies by ROMP, i.e., bottlebrush polymers, choice of anchor group becomes critical to reach high degrees of polymerization and achieve low dispersity polymers, a topic we are currently investigating in our laboratory.

#### ASSOCIATED CONTENT

## **Supporting Information**

Supporting Information: Monomer synthesis, NMR spectra, kinetics graphs, SEC traces, HOMO energies, and monomer coordinates (PDF)

#### **AUTHOR INFORMATION**

#### **Corresponding Author**

John B. Matson – Department of Chemistry and Macromolecules Innovation Institute, Virginia Tech, Blacksburg 24061 Virginia, United States

## **Authors**

Samantha J. Scannelli – Department of Chemistry and Macromolecules Innovation Institute, Virginia Tech, Blacksburg 24061 Virginia, United States

Anshul Paripati – Department of Chemistry and Macromolecules Innovation Institute, Virginia Tech, Blacksburg 24061 Virginia, United States

Jeffrey R. Weaver – Department of Chemistry and Macromolecules Innovation Institute, Virginia Tech, Blacksburg 24061 Virginia, United States

Clark Vu – Department of Chemistry and Macromolecules Innovation Institute, Virginia Tech, Blacksburg 24061 Virginia, United States

Mohammed Alaboalirat – Department of Chemistry and Macromolecules Innovation Institute,

Virginia Tech, Blacksburg 24061 Virginia, United States

Current Address: Research and Development Center, Saudi Aramco, Dhahran 31311, Saudi Arabia

Diego Troya – Department of Chemistry and Macromolecules Innovation Institute, Virginia Tech, Blacksburg 24061 Virginia, United States

#### Notes

The authors declare no competing financial interest.

#### **ACKNOWLEDGMENTS**

This work was supported by a joint grant between the National Science Foundation and the Binational Science Foundation (DMR-2104602) and by GlycoMIP, a National Science Foundation Materials Innovation Platform funded through Cooperative Agreement DMR-1933525. We thank Dr. Santu Sarkar, and Tamalika Paul for critical reading of the manuscript. We also thank Dr. Narasimhamurthy Shanaiah for helpful suggestions pertaining to our NMR experiments. The authors acknowledge Advanced Research Computing at Virginia Tech for providing computational resources and technical support that have contributed to the results reported within this paper. We also acknowledge the Virginia Tech Mass Spectrometry Research Incubator for high-resolution mass spectrometry analysis.

#### REFERENCES

- 1. Szwarc, M., Living polymers. Their discovery, characterization, and properties. *J. Polym. Sci., Part A: Polym. Chem.* **1998**, *36*, IX-XV.
- 2. Stenzel, M. H.; Barner-Kowollik, C., The living dead common misconceptions about reversible deactivation radical polymerization. *Mater. Horiz.* **2016**, *3*, 471-477.
- 3. Nicolaÿ, R.; Kwak, Y.; Matyjaszewski, K., A Green Route to Well-Defined High-Molecular-Weight (Co)polymers Using ARGET ATRP with Alkyl Pseudohalides and Copper Catalysis. *Angew. Chem* **2010**, *49*, 541-544.
- 4. Carmean, R. N.; Sims, M. B.; Figg, C. A.; Hurst, P. J.; Patterson, J. P.; Sumerlin, B. S., Ultrahigh Molecular Weight Hydrophobic Acrylic and Styrenic Polymers through Organic-Phase Photoiniferter-Mediated Polymerization. *ACS Macro Lett.* **2020**, *9*, 613-618.
- 5. Gody, G.; Maschmeyer, T.; Zetterlund, P. B.; Perrier, S., Rapid and quantitative one-pot synthesis of sequence-controlled polymers by radical polymerization. *Nat. Commun.* **2013**, *4*, 2505.
- 6. Steube, M.; Johann, T.; Galanos, E.; Appold, M.; Rüttiger, C.; Mezger, M.; Gallei, M.; Müller, A. H. E.; Floudas, G.; Frey, H., Isoprene/Styrene Tapered Multiblock Copolymers with up to Ten Blocks: Synthesis, Phase Behavior, Order, and Mechanical Properties. *Macromolecules* **2018**, *51*, 10246-10258.
- 7. Eugene, D. M.; Grayson, S. M., Efficient Preparation of Cyclic Poly(methyl acrylate)-block-poly(styrene) by Combination of Atom Transfer Radical Polymerization and Click Cyclization. *Macromolecules* **2008**, *41*, 5082-5084.
- 8. Jia, Z.; Monteiro, M. J., Cyclic polymers: Methods and strategies. *J. Polym. Sci., Part A: Polym. Chem.* **2012**, *50*, 2085-2097.

- 9. Matyjaszewski, K., The synthesis of functional star copolymers as an illustration of the importance of controlling polymer structures in the design of new materials. *Polym. Int.* **2003**, *52*, 1559-1565.
- 10. Jha, S.; Dutta, S.; Bowden, N. B., Synthesis of Ultralarge Molecular Weight Bottlebrush Polymers Using Grubbs' Catalysts. *Macromolecules* **2004**, *37*, 4365-4374.
- 11. Sheiko, S. S.; Sumerlin, B. S.; Matyjaszewski, K., Cylindrical molecular brushes: Synthesis, characterization, and properties. *Prog. Polym. Sci.* **2008**, *33*, 759-785.
- 12. Radzinski, S. C.; Foster, J. C.; Scannelli, S. J.; Weaver, J. R.; Arrington, K. J.; Matson, J. B., Tapered Bottlebrush Polymers: Cone-Shaped Nanostructures by Sequential Addition of Macromonomers. *ACS Macro Lett.* **2017**, *6*, 1175-1179.
- 13. Li, A.; Li, Z.; Zhang, S.; Sun, G.; Policarpio, D. M.; Wooley, K. L., Synthesis and Direct Visualization of Dumbbell-Shaped Molecular Brushes. *ACS Macro Lett.* **2012**, *1*, 241-245.
- 14. Walsh, D. J.; Guironnet, D., Macromolecules with programmable shape, size, and chemistry. *Proc. Natl. Acad. Sci.* **2019**, *116*, 1538-1542.
- 15. Jenkins, A. D.; Kratochvíl, P.; Stepto, R. F. T.; Suter, U. W., Glossary of basic terms in polymer science (IUPAC Recommendations 1996). *Pure Appl. Chem.* **1996**, *68*, 2287-2311.
- 16. Szwarc, M., 'Living' Polymers. *Nature* **1956**, *178*, 1168-1169.
- 17. Matyjaszewski, K., Ranking living systems. *Macromolecules* **1993**, *26*, 1787-1788.
- 18. Grubbs, R. B.; Grubbs, R. H., 50th Anniversary Perspective: Living Polymerization—Emphasizing the Molecule in Macromolecules. *Macromolecules* **2017**, *50*, 6979-6997.
- 19. Matyjaszewski, K., Atom Transfer Radical Polymerization (ATRP): Current Status and Future Perspectives. *Macromolecules* **2012**, *45*, 4015-4039.
- 20. Keddie, D. J.; Moad, G.; Rizzardo, E.; Thang, S. H., RAFT Agent Design and Synthesis. *Macromolecules* **2012**, *45*, 5321-5342.
- 21. Bielawski, C. W.; Grubbs, R. H., Living ring-opening metathesis polymerization. *Prog. Polym. Sci.* **2007**, *32*, 1-29.
- 22. Blosch, S. E.; Scannelli, S. J.; Alaboalirat, M.; Matson, J. B., Complex Polymer Architectures Using Ring-Opening Metathesis Polymerization: Synthesis, Applications, and Practical Considerations. *Macromolecules* **2022**, *55*, 4200-4227.
- 23. Hilf, S.; Kilbinger, A. F. M., Sacrificial Synthesis of Hydroxy-Telechelic Metathesis Polymers via Multiblock-Copolymers. *Macromolecules* **2009**, *42*, 1099-1106.
- 24. Liu, J.; Li, J.; Xie, M.; Ding, L.; Yang, D.; Zhang, L., A novel amphiphilic AB2 star copolymer synthesized by the combination of ring-opening metathesis polymerization and atom transfer radical polymerization. *Polymer* **2009**, *50*, 5228-5235.
- 25. Choi, T.-L.; Grubbs, R. H., Controlled Living Ring-Opening-Metathesis Polymerization by a Fast-Initiating Ruthenium Catalyst. *Angew. Chem* **2003**, *42*, 1743-1746.
- 26. Radzinski, S. C.; Foster, J. C.; Chapleski, R. C.; Troya, D.; Matson, J. B., Bottlebrush Polymer Synthesis by Ring-Opening Metathesis Polymerization: The Significance of the Anchor Group. *J. Am. Chem. Soc.* **2016**, *138*, 6998-7004.
- 27. Slugovc, C.; Demel, S.; Riegler, S.; Hobisch, J.; Stelzer, F., The Resting State Makes the Difference: The Influence of the Anchor Group in the ROMP of Norbornene Derivatives. *Macromol. Rapid Commun.* **2004**, *25*, 475-480.
- 28. Pollino, J. M.; Stubbs, L. P.; Weck, M., Living ROMP of exo-Norbornene Esters Possessing PdII SCS Pincer Complexes or Diaminopyridines. *Macromolecules* **2003**, *36*, 2230-2234.

- 29. Rule, J. D.; Moore, J. S., ROMP Reactivity of endo- and exo-Dicyclopentadiene. *Macromolecules* **2002**, *35*, 7878-7882.
- 30. Becke, A. D., Density-functional thermochemistry. III. The role of exact exchange. *J. Chem. Phys.* **1993**, *98*, 5648-5652.
- 31. Stephens, P. J.; Devlin, F. J.; Chabalowski, C. F.; Frisch, M. J., Ab Initio Calculation of Vibrational Absorption and Circular Dichroism Spectra Using Density Functional Force Fields. *J. Phys. Chem.* **1994**, *98*, 11623-11627.
- 32. Zhao, Y.; Truhlar, D. G., The M06 suite of density functionals for main group thermochemistry, thermochemical kinetics, noncovalent interactions, excited states, and transition elements: two new functionals and systematic testing of four M06-class functionals and 12 other functionals. *Theor. Chem. Acc.*, **2008**, *120*, 215-241.
- 33. Weigend, F.; Ahlrichs, R., Balanced basis sets of split valence, triple zeta valence and quadruple zeta valence quality for H to Rn: Design and assessment of accuracy. *Phys. Chem. Phys.* **2005**, *7*, 3297-3305.
- 34. Walsh, D. J.; Lau, S. H.; Hyatt, M. G.; Guironnet, D., Kinetic Study of Living Ring-Opening Metathesis Polymerization with Third-Generation Grubbs Catalysts. *J. Am. Chem. Soc.* **2017**, *139*, 13644-13647.
- 35. Bielawski, C. W.; Grubbs, R. H., Highly Efficient Ring-Opening Metathesis Polymerization (ROMP) Using New Ruthenium Catalysts Containing N-Heterocyclic Carbene Ligands. *Angew. Chem* **2000**, *39*, 2903-2906.
- 36. Hyatt, M. G.; Walsh, D. J.; Lord, R. L.; Andino Martinez, J. G.; Guironnet, D., Mechanistic and Kinetic Studies of the Ring Opening Metathesis Polymerization of Norbornenyl Monomers by a Grubbs Third Generation Catalyst. *J. Am. Chem. Soc.* **2019**, *141*, 17918-17925.
- 37. Suresh, C. H.; Koga, N., Orbital Interactions in the Ruthenium Olefin Metathesis Catalysts. *Organometallics* **2004**, *23*, 76-80.
- 38. Zografos, A.; Lynd, N. A.; Bates, F. S.; Hillmyer, M. A., Impact of Macromonomer Molar Mass and Feed Composition on Branch Distributions in Model Graft Copolymerizations. *ACS Macro Lett.* **2021**, *10*, 1622-1628.
- 39. Blosch, S. E.; Alaboalirat, M.; Eades, C. B.; Scannelli, S. J.; Matson, J. B., Solvent Effects in Grafting-through Ring-Opening Metathesis Polymerization. *Macromolecules* **2022**, *55*, 3522-3532.
- 40. Wolf, W. J.; Lin, T.-P.; Grubbs, R. H., Examining the Effects of Monomer and Catalyst Structure on the Mechanism of Ruthenium-Catalyzed Ring-Opening Metathesis Polymerization. *J. Am. Chem. Soc.* **2019**, *141*, 17796-17808.
- 41. Trnka, T. M.; Grubbs, R. H., The Development of L2X2RuCHR Olefin Metathesis Catalysts: An Organometallic Success Story. *Acc. Chem. Res.* **2001**, *34*, 18-29.
- 42. Jawiczuk, M.; Marczyk, A.; Trzaskowski, B., Decomposition of Ruthenium Olefin Metathesis Catalysts **2020**, *10*, 887.
- 43. O'Haver, T. *peakfit.m*, 8.2; https://www.mathworks.com/matlabcentral/fileexchange/23611-peakfit-m, 2022.
- 44. Matos, J. M. E.; Lima-Neto, B. S., Benefits of donor solvents as additive on ROMP of norbornene catalyzed by amine Ru complexes. *J. Mol. Catal. A Chem.* **2005**, *240*, 233-238.
- 45. Foster, J. C.; Grocott, M. C.; Arkinstall, L. A.; Varlas, S.; Redding, M. J.; Grayson, S. M.; O'Reilly, R. K., It is Better with Salt: Aqueous Ring-Opening Metathesis Polymerization at Neutral pH. *J. Am. Chem. Soc.* **2020**, *142*, 13878-13885.